Electrocatalysis (2019) 10:203–213
https://doi.org/10.1007/s12678-019-00515-8

ORIGINAL RESEARCH

The Catalytic Activity of Pt:Ru Nanoparticles for Ethylene Glycol and Ethanol Electrooxidation in a Direct Alcohol Fuel Cell

Júlio César M. Silva[1] · Spyridon Ntais[2] · Vishwanathan Rajaraman[2] · Érico Teixeira-Neto[3] · Ângela A. Teixeira-Neto[3] · Almir O. Neto[4] · Rodolfo M. Antoniassi[4] · Estevam V. Spinacé[4] · Elena A. Baranova[2]

Published online: 8 March 2019

Abstract

In this study, we investigated the carbon-supported PtRu nanoparticles with atomic ratios of Pt:Ru of 100:0, 90:10, 70:30, and 50:50 for ethanol and ethylene glycol electrooxidation in alkaline media. The nanoparticles were synthesized using sodium borohydride method with 20 wt% of metals loading on carbon. The nanoparticle mean sizes were 7.3 nm, 5.7 nm, 5.2 nm, and 5.1 nm for Pt/C, $Pt_{90}Ru_{10}$/C, $Pt_{70}Ru_{30}$/C, and $Pt_{50}Ru_{50}$/C, respectively. X-ray diffraction (XRD) analysis revealed that Pt and PtRu electrocatalysts have face-centered cubic (fcc) structure and suggests the alloy formation for all PtRu/C materials, which was further supported by the X-ray photoelectron spectroscopy (XPS). Based on XPS analysis, $Pt_{50}Ru_{50}$/C has higher amount of Pt oxides on the surface than $Pt_{70}Ru_{30}$/C. Electrochemical results demonstrated that the addition of Ru to Pt enhances the catalytic activity towards ethanol and ethylene glycol electrooxidadion. The catalyst of $Pt_{50}Ru_{50}$/C composition showed the lowest onset potential for ethanol and ethylene glycol electrooxidation, which were 160 and 70 mV lower than for Pt/C, respectively. Furthermore, this catalyst outperformed Pt/C and other PtRu/C compositions in chronoamperometric and direct alcohol fuel cell (DAFC) experiments. DAFC experiments using $Pt_{50}Ru_{50}$/C as anode had the power density 40 and 14% higher than using Pt/C for ethanol and ethylene glycol, respectively. The promotion is due to the bi-functional mechanism and/or electronic effect of two metals in the alloy.

Keywords PtRu nanoparticles · Ethanol · Ethylene glycol · Direct alcohol fuel cell · Electronic effect

Introduction

The use of excessive fossil fuels has resulted in harmful effects on the environment and potentially human health. The concentration of CO_2 in the atmosphere has recently surpassed the 400 ppm threshold for the first time in modern history [1]. In this context, fuel cells may offer an excellent alternative to the current fossil fuel-based energy generation technologies as clean and efficient power sources [2]. Considering these aspects, fuel cells represent an attractive alternative for transport and stationary power generation, and this technology could contribute to the reduction of greenhouse gas emissions produced from fossil fuels [3].

Liquid fuels are considerably more convenient in terms of handling and transportation if compared to gaseous hydrogen [4]. In this sense, direct alcohol fuel cells DAFCs are promising energy-producing devices that comprise alcohol, e.g., methanol, ethanol, ethylene glycol, glycerol, etc. electrooxidation at the anode and oxygen reduction reaction at the cathode [5–8]. Bioethanol and ethylene glycol from biomass [5, 9–11] are appealing fuels for DAFCs due to their lower toxicity and high theoretical energy density, 8.01 kWh kg^{-1} and 5.2 kWh kg^{-1}, respectively [12]. The complete electrooxidation to CO_2 involves 12 electrons for ethanol molecule, and 10 electrons for ethylene glycol molecule [5, 11]; however, the complete oxidation of ethanol and ethylene glycol to CO_2 requires the C–C bond splitting, which

✉ Júlio César M. Silva
quimijulio@gmail.com

✉ Elena A. Baranova
elena.baranova@uottawa.ca

[1] Grupo de Eletroquímica e Materiais Nanoestruturados, Campus Valonguinho, Instituto de Química da Universidade Federal Fluminense, Niterói, RJ CEP 24020-141, Brazil

[2] Department of Chemical and Biological Engineering, Centre for Catalysis Research and Innovation (CCRI), University of Ottawa, 161 Louis-Pasteur, Ottawa, ON K1N 6N5, Canada

[3] Brazilian Nanotechnology National Laboratory, Brazilian Center for Research in Energy and Materials, Rua Giuseppe Máximo Scolfaro, 10.000, Campinas, SP 13085-903, Brazil

[4] Instituto de Pesquisas Energéticas e Nucleares, IPEN/CNEN-SP, Av. Prof. Lineu Prestes, 2242 Cidade Universitaria, São Paulo, SP CEP 05508-900, Brazil

is hindered at low temperatures [6, 13–15]. The main products of ethanol electrooxidation are acetaldehyde and acetic acid (acetate in alkaline media) [14, 16]. The oxidation of ethanol to acetate involves an exchange of four electrons per molecule of ethanol [17, 18], which corresponds to Faradaic efficiency of 33.3%. Similarly, for ethylene glycol, oxalate is the dominant product [6, 15], which involves eight electrons per molecule of ethylene glycol corresponding to a Faradaic efficiency of 80% [19, 20]. Higher efficiency in terms of number of electrons per molecule is obtained for the incomplete oxidation of ethylene glycol to oxalate than when ethanol is oxidized to acetate. Alkaline media offers some advantages in comparison with acid media, like higher kinetics of the oxygen reduction reaction (ORR) and alcohol oxidation, use of less expensive catalysts, as well as the less corrosive nature of an alkaline environment ensures a potential greater longevity of the fuel cell [21].

Platinum is one of the most studied electrocatalysts for oxidation of small organic molecules due its high catalytic activity and stability [13, 22]; however, Pt shows inability to efficiently split the C-C in ethanol and ethylene glycol and suffers from deactivation by poisoning intermediates towards ethanol electrooxidation [5, 6, 10, 13, 15, 22–25]. To overcome these issues, Pt-based bimetallic and multimetallic materials such as PtAu [13, 26], PtSn [17, 24], PtBi [27, 28], PtSnRu [5, 10], and others are actively being pursued by various research groups.

Ethylene glycol electrooxidation in acidic and alkaline media using PtRu as electrocatalysts has been reported previously [5, 6, 10]. Falase et al. [5] synthesized $Pt_{84}Ru_{16}$, $Pt_{96}Sn_4$ and $Pt_{88}Ru_6Sn_6$ using spray pyrolysis approach and evaluated the materials towards ethylene glycol electrooxidation in KOH. They reported that $Pt_{84}Ru_{16}$ had the best catalytic activity due to CO_2 production at lower overpotentials: 0.73 V vs 0.84 for $Pt_{96}Sn_4$ and $Pt_{88}Ru_6Sn_6$, respectively.

Hyung Ju Kim et al. [10] reported the results of ethylene glycol electrooxidation in acid media using Pt/C, Pt_5Ru_5/C, and $Pt_5Ru_4Sn_1$/C electrocatalysts prepared by colloidal method. The bimetallic and ternary materials showed better catalytic activity compared to monometallic Pt/C. However, in these two studies, the influence of the different atomic ratios between Pt and Ru were not evaluated.

PtRu electrocatalysts for ethanol electrooxidation in acid media have been widely investigated and reported in several previous works [6, 29–32]. The beneficial effect of adding Ru to Pt for ethanol and ethylene glycol electrooxidation has been reported previously [29, 33, 34]. The enhancement in the catalytic activity of Pt by adding Ru is ascribed as ligand effect (electronic effect) and bi-functional mechanism. The ligand effect is based on the modification of the electronic structure of Pt which weakens the bond strength of poisoning intermediates on the Pt surface [29, 33, 34]. According to the bi-functional mechanism, Ru could provide oxygen species from water activation (Ru—OH) to oxidize adsorbed (poisoning species) intermediate species from the oxidation of ethanol and ethylene glycol [29, 33, 34].

There are less reports on ethanol electrooxidation on PtRu in alkaline solution. Kanninen et al. [35] have reported results on ethanol electrooxidation in alkaline media on PtRu electrocatalysts; the main purpose of the study was to investigate the influence of the three differently modified few-walled carbon nanotubes on the catalytic performance.

Despite the fact that various PtRu nanoparticles were investigated for ethanol and ethylene glycol oxidation in acid and alkaline media, to the best of our knowledge, there are no works that report the effect of the various Pt:Ru atomic composition on ethanol and ethylene glycol oxidation reaction in alkaline media in the three-electrode electrochemical cell and fuel cell configuration, whereas this parameter could significantly affect the catalyst performance and durability. It is well known that electrocatalytic activity, stability, and in some cases selectivity strongly depend on the method of nanoparticle preparation, ratio between metals in multimetallic catalysts, their size, particle size distribution, type of the support, and surface and bulk composition of the active phase. Therefore, these parameters need to be investigated to establish the structure to property correlation for the design of active and selective electrocatalysts.

In the present work, Pt_xRu_{1-x}/C with $x = 100$, 90, 70 and 50 at. % were synthesized using sodium borohydride reduction method and studied for ethanol and ethylene glycol electrooxidation in alkaline media in order to find the optimum Pt to Ru ratio and correlate the bulk and surface composition with the catalytic activity. Detailed physicochemical characterizations (XRD, STEM, XPS) of Pt_xRu_{1-x}/C nanoparticles as well as electrochemical and fuel cell experiments with both alcohols were carried out to elucidate the role of adding Ru to Pt and to confirm the applicability of these anode materials in DAFC.

Experimental

Nanoparticle Synthesis

The PtRu/C electrocatalyts (20 wt% of metal loading) with different atomic ratios of 100:0, 90:10, 70:30, 50:50 were prepared by the sodium borohydride reduction process reported earlier [36, 37]. In the synthesis process, $H_2PtCl_6{\cdot}6H_2O$ (Aldrich) and ruthenium (III) chloride (Aldrich) were used. All reagents were analytical grade. In the synthesis, carbon black (Cabot, Vulcan XC-72) was first dispersed in isopropanol//water solution (50/50, *v*/*v*). The mixture was homogenized under stirring and then the metal precursor salts were added and placed in an ultrasonic bath for 5 min. Then, 10 mL of 0.15 M $NaBH_4$ (Aldrich) in 0.1 mol L^{-1} KOH was

added in one portion under vigorous stirring at room temperature. The resulting colloidal solution was stirred for 15 min to allow the completion of the reaction and then solids were filtered and washed with deionized (DI) water (Milli-Q® Millipore, 18.2 MΩ cm at 293 K) and finally dried at 70 °C for 2 h.

Physicochemical Characterization

The morphology and nanoparticle size distribution were determined by transmission electron microscopy (TEM) analysis using a JEOL transmission electron microscope model JEM-2100 operated at STEM (scanning transmission electron microscope) mode. The nanoparticle size was achieved by counting about 200 particles at different regions of the materials. The actual atomic composition of Pt and Ru in the synthesized materials was measured by energy-dispersive spectroscopy (EDS) using a JEOL-JSM6010 LA equipment.

The crystal structure of the nanoparticles was characterized by X-ray diffraction (XRD) using a Rigaku diffractometer model Miniflex II using Cu Kα radiation source (0.15406 nm). The X-ray diffraction patterns were recorded in the range of 20° to 90° 2θ with a step size of 0.05° and a scan time of 2 s per step.

The X-ray photoelectron spectroscopy (XPS) analysis was carried out with an SPECSLAB II (Phoibos-Hsa 3500 150, 9 channeltrons) SPECS spectrometer, with Al Kα source (E = 1486.6 eV) working at 15 kV, Epass = 40 eV, 0.2 eV energy step, and 2 s per point was the acquisition time. The deconvolution of the Pt4f peak was performed using doublets with spin orbit splitting 3.35 eV and intensity ratio $Pt4f_{7/2}$:$Ptf_{5/2}$ = 4/3 while a peak asymmetry was used in the case of the Pt4f peaks attributed to the metallic based on the work of Hufner et al. [38]. Binding energy scale was corrected using C1S XPS peak at 284.6 eV as an internal standard.

Electrochemical Characterization

Electrochemical measurements were carried out using a PARSTAT 2263 (Princeton Applied Research) in a conventional three-electrode electrochemical cell made of Teflon at room temperature, unless otherwise stated. A large surface platinum gauze and Hg/HgO (Koslow Scientific) were used as the counter and reference electrodes, respectively. Nanoparticle catalysts were deposited on glassy carbon (GC) electrode (0.166 cm^2 of geometric area). Before each experiment, the GC support was polished with alumina suspension (1 μm) and washed in deionized water. Ultrapure deionized water obtained from a Milli-Q system (Millipore®, 18.2 MΩ cm at 293 K) was used in all experimental procedures.

The catalyst "ink" was prepared by dispersing 6 mg of the electrocatalyst powder in 1 mL DI water, 100 μL isopropanol, and mixing for 15 min in an ultrasonic bath. Shortly thereafter, 100 μL of 5% Nafion® solution was added to the suspension, which was mixed again for 20 min in an ultrasonic bath. Aliquots of 8 μL of the dispersion fluid were pipetted onto the GC surface. Finally, the electrode was dried at 60 °C for 20 min.

Cyclic voltammograms (CVs) were carried out at a scan rate of 20 mV s^{-1} between − 0.85 and 0.2 V vs. Hg/HgO. The electrocatalysts were cycled for ten consecutive cycles in 1 mol L^{-1} KOH and for five consecutive cycles in alcohol containing solutions. Chronoamperometric experiments were carried out for 1 h at − 0.35 V vs Hg/HgO. The electrooxidation of ethanol and ethylene glycol was performed in a 1 mol L^{-1} KOH and 1 mol L^{-1} alcohol solution.

The electrochemical active surface area (ECSA) of the catalysts was determined by CO stripping experiments, integrating the CO_{ad} stripping charges, assuming the factor of 420 μC cm^{-2} [39]. In this procedure, a mixture of CO (1%) and He (99%) was bubbled into 1 mol L^{-1} KOH solution for 20 min while holding the working electrode at − 0.6 V, then pure N_2 was bubbled instead of the gas mixture for 20 min to remove the dissolved CO in the solution. The CO stripping voltammograms were then recorded at a scan rate of 20 mVs^{-1}. The ethanol and ethylene glycol current from electrochemical experiments were normalized per ECSA obtained by CO stripping. All electrochemical measurements were carried out at room temperature unless otherwise stated.

Fuel Cell Performance Measurements

DAFCs experiments were conducted as already described elsewhere [13, 18]. In these experiments, a single cell set at 70 °C with an electrode area of 5 cm^2 was employed. The temperature of the oxygen humidifier was maintained at 85 °C. The cathode was a commercial Pt/C (BASF) and anode was Pt_xRu_{1-x} (x = 100, 90, 70, and 50 at%) prepared in the present work. The cathode had Pt loading of 2 mg cm^{-2} and anodes of 1 mg of PtRu per cm^2. A Nafion® 117 membrane previously exposed to 6 mol L^{-1} KOH for 24 h [13, 18, 40, 41] was used for the fuel cell experiments.

Results and Discussion

Physical Chemical Characterization

Figure 1 shows the micrographs and histograms of the particle mean diameter distributions for Pt/C and binary PtRu/C materials. For Pt/C (Fig. 1a) in addition to well-dispersed NPs, some particle aggregates can be seen. The Pt/C histogram shows a broad size distribution that ranges from 2 to 32 nm, and about 18% of the nanoparticles have diameter higher than 10 nm. For $Pt_{90}Ru_{10}$/C, although some aggregations can be

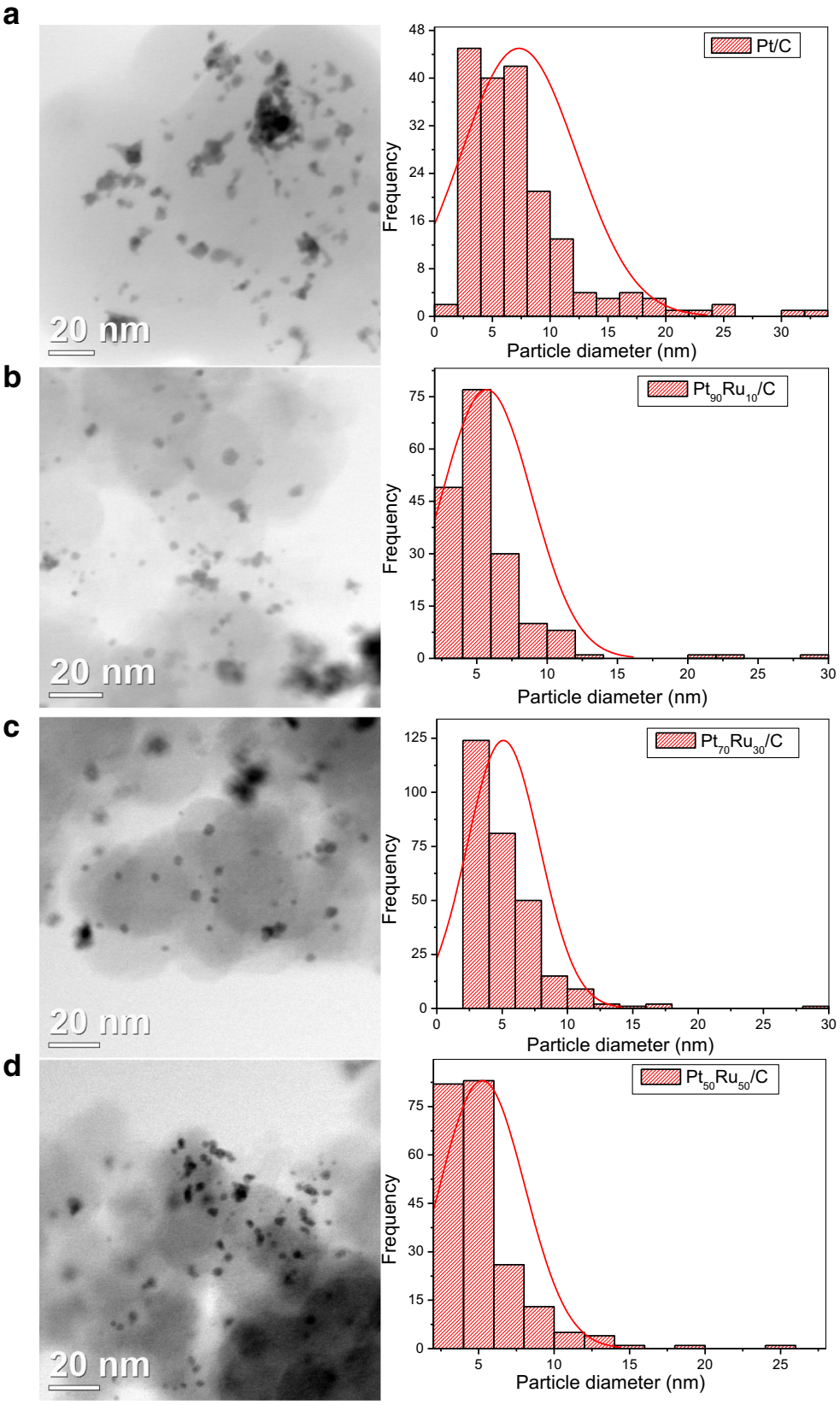

Fig. 1 The STEM micrographs and corresponding histograms of Pt/C (**a**), $Pt_{90}Ru_{10}$/C (**b**), $Pt_{70}Ru_{30}$/C (**c**) and $Pt_{50}Ru_{50}$/C (**d**)

seen in Fig. 1b, approximately 93% of the nanoparticles are smaller than 10 nm as can be observed in the histogram. The $Pt_{70}Ru_{30}$/C (Fig. 1c) and $Pt_{50}Ru_{50}$/C (Fig. 1d) nanoparticle sizes are similar to the $Pt_{90}Ru_{10}$/C. The mean diameter of

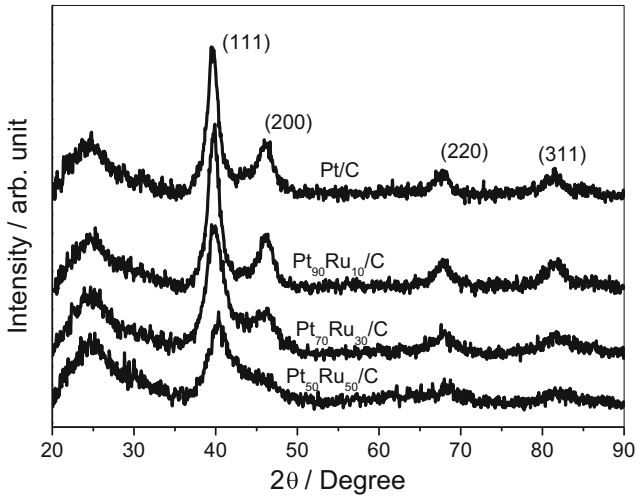

Fig. 2 X-ray diffraction patterns for the Pt/C and PtRu/C electrocatalysts

the nanoparticles from STEM micrographs are 7.3 nm, 5.7 nm, 5.2 nm, and 5.1 nm for Pt/C, $Pt_{90}Ru_{10}$/C, $Pt_{70}Ru_{30}$/C, and $Pt_{50}Ru_{50}$/C, respectively. This indicates that addition of Ru decreases the particle size of Pt. The heterogeneity present in the nanoparticle sizes is typical for the sodium borohydride preparation method [13, 18, 40, 42]; however, despite broad size distribution, this method is well-suited for fuel cell catalyst preparation as it is straightforward and easy to scale up method.

X-ray diffraction patterns of the carbon-supported platinum and bimetallic PtRu nanoparticles are shown in Fig. 2. In all XRD patterns, a broad peak at about 25° 2θ is due to the (022) reflection of the hexagonal structure of carbon black (Vulcan XC 72) [43, 44]. The face-centered cubic (fcc) structure of Pt can be observed by the peaks at approximately 39°, 46°, 67°, and 81° 2θ [44, 45]. The diffraction peaks of PtRu catalysts are shifted to higher 2θ values if compared to the same reflections of Pt/C (Table 1) suggesting the PtRu alloy formation [46, 47] and the shift increases with the atomic composition of Ru. In accordance with the Vegard's law, Ru incorporates to Pt-forming fcc structure up to 70 at%. For $Pt_{50}Ru_{50}$ catalysts, only a single 111 reflection is observed at 40.37° 2θ similar to the previous work [46, 47]. The crystallite size, estimated using Scherrer equation and (220) peak [2, 43], and the actual composition of all PtRu/C electrocatalysts obtained by the EDS analysis are summarized in Table 1.

The crystallite sizes of the material with high amount of ruthenium were lower than the material with only 10% of rutheium and Pt/C, which is in agrement with STEM data. The actual atomic composition obtained by EDS analysis was very close to the nominal one.

The analysis of Pt4f XPS peak of carbon-supported $Pt_{50}Ru_{50}$ and $Pt_{70}Ru_{30}$ revealed the existence of three components. For the $Pt_{50}Ru_{50}$, the deconvoluted components at 71.5 (Pt^{I}), 72.2 (Pt^{II}), and 73.7 eV (Pt^{III}) are attributed to Pt^0, Pt^{2+}, and Pt^{4+}, respectively [48–50]. In the case of $Pt_{70}Ru_{30}$ sample, a negative shift towards lower BEs is observed mainly for the component attributed to the metallic state. A similar trend was observed in our previous study and was attributed to the alloy formation between Pt and Ru [2]. For the $Pt_{50}Ru_{50}$ catalyst, the Ru3p XPS peak is detected at 462.3 eV, while a small shift towards higher BEs (~0.15 eV) is observed for the corresponding peak in $Pt_{70}Ru_{30}$ sample. This BE is characteristic of Ru^{4+}, e.g., in RuO_2 [51]; however, due to the large width of the recorded peaks, we cannot exclude the presence of ruthenium in metallic state or as hydrated species, etc. [52, 53]. Moreover, the Ru3p XPS peak in the case of the $Pt_{50}Ru_{50}$ shows a shoulder around 466.2 eV which corresponds to hydrated ruthenium species [54] and its existence strongly suggests the presence of relatively high amounts of RuO_2xH_2O in this sample. On the other hand, in the case of the $Pt_{70}Ru_{30}$ catalyst, no such pronounced contribution due to hydrated species is found (Fig. 3).

Table 2 summarizes the position and the relative intensities of the XPS peak components of the two catalysts. The observed shifts are attributed to an alloy formation where an electron transfer from ruthenium towards platinum atoms takes place. This electron transfer increases the electron density around Pt atoms as the Ru content increases thus shifting the Pt4f XPS peak to lower BEs. Our results also imply that the Pt/Ru content affects the abundance of hydrated ruthenium species, whereas no significant differences are detected on the abundance of platinum atoms with different oxidation states. Based on the intensities of the XPS peaks, the Pt/Ru surface atomic ratios were calculated for both samples. In the case of the $Pt_{50}Ru_{50}$ sample, the ratio was found to be 0.97 in accordance with the nominal ratio, while for the $Pt_{70}Ru_{30}$, it was found to be 3.1 compared to 2.33 for the nominal bulk

Table 1 Characteristics of carbon-supported Pt and PtRu catalysts

Electrocatalyst nominal at. %	Atomic composition (%) from EDS	Crystallite size from (220) (nm)	2 θ_{max} of (111) (°)	ECSA (cm^2)
Pt/C	–	4.3	39.64	0.76
$Pt_{90}Ru_{10}$/C	90:10	4.5	39.79	0.98
$Pt_{70}Ru_{30}$/C	69:31	3.6	39.85	0.77
$Pt_{50}Ru_{50}$/C	51:49	3.3	40.37	0.42

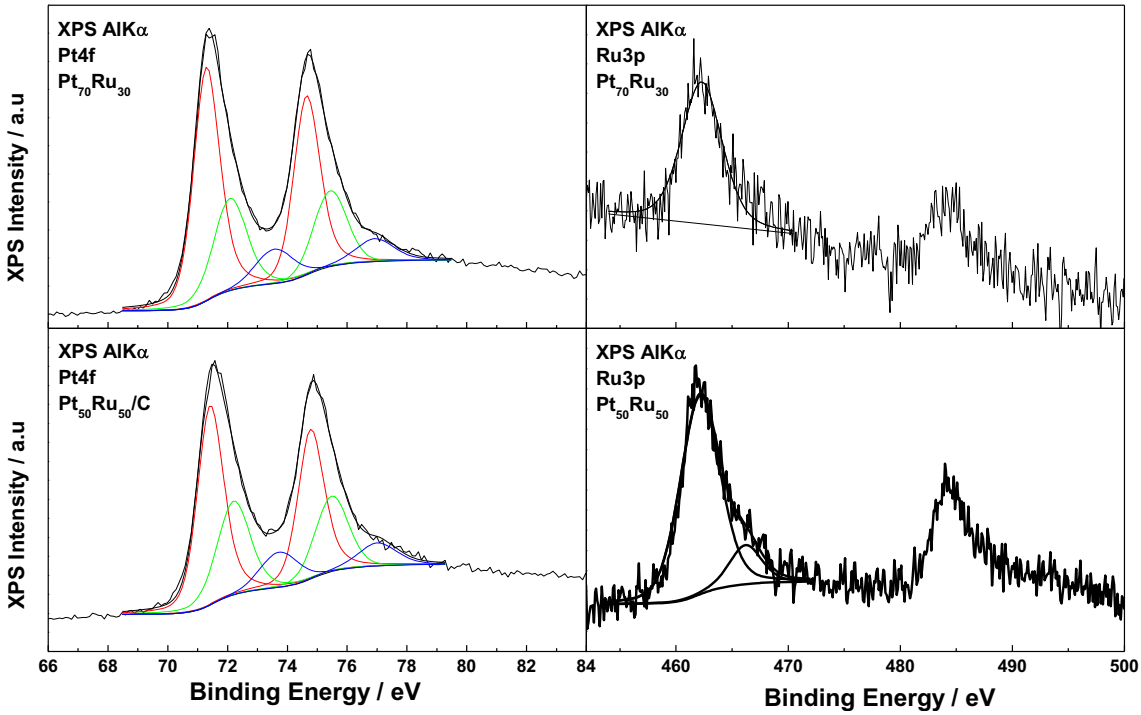

Fig. 3 X-ray photoelectron spectra of Pt4f levels (left spectra) and Ru3p (right spectra) of the carbon-supported $Pt_{50}Ru_{50}$ and the $Pt_{70}Ru_{30}$ as indicated in the figure

atomic ratio. This indicates a Pt surface enrichment for $Pt_{70}Ru_{30}$ catalysts.

Electrochemical Measurements

The results of the CV experiments in 1 mol L^{-1} KOH for all electrocatalysts in the potential region between − 0.85 V and 0.2 V are shown in Fig. 4. As can be seen for Pt/C, there are two peaks related to the hydrogen adsorption/desorption process at about −0.63 and − 0.53 V [45, 55]. The region from − 0.20 to 0.2 V is associated with the formation of an oxide layer on the platinum surface [17, 45]. The reduction of oxides on platinum surface occurs at about − 0.18 V as can be seen in the reversible scan [45, 56]. As the Ru content increases in PtRu/C electrocatalysts, the charging current increases. This increase is characteristic of Ru as was reported for acidic and alkaline solutions [57]. For $Pt_{70}Ru_{30}$/C and $Pt_{50}Ru_{50}$/C, the two peaks related to hydrogen adsorption/desorption process are not well defined as the surface is Ru enriched, and this behavior has been already reported for PtRu/C electrocatalysts with high amount of Ru in the materials [55, 58].

Ethanol Electrooxidation

Figure 5 shows the cyclic voltammograms of ethanol electrooxidation on Pt_xRu_{100-x}/C ($x = 100$, 90, 70, and 50 at.%) in 1 mol L^{-1} KOH + 1 mol L^{-1} ethanol. The lowest onset potential of ~ − 0.60 V vs Hg/HgO was obtained on $Pt_{50}Ru_{50}$/C, whereas it increases as the amount of Ru decreases and is − 0.56, − 0.51, and − 0.44 V for $Pt_{70}Ru_{30}$/C, $Pt_{90}Ru_{10}$/C,

Table 2 XPS characteristics of Pt $4f_{7/2}$ and Ru $3p_{3/2}$ peaks

Catalyst	$Pt4f_{7/2}$			Ru $3p_{3/2}$	Pt/Ru surface at. ratio from XPS	Pt/Ru nominal at. ratio
	B.E. (eV)	% Relative intensities	Assignment	BE (eV)		
$Pt_{50}Ru_{50}$	71.5	56	Metallic Pt	462.2	0.97	1
	72.2	32	Pt^{2+}	466.2		
	73.7	12	Pt^{4+}			
$Pt_{70}Ru_{30}$	71.3	61	Metallic Pt	462.3	3.1	2.33
	72.1	29	Pt^{2+}			
	73.7	10	Pt^{4+}			

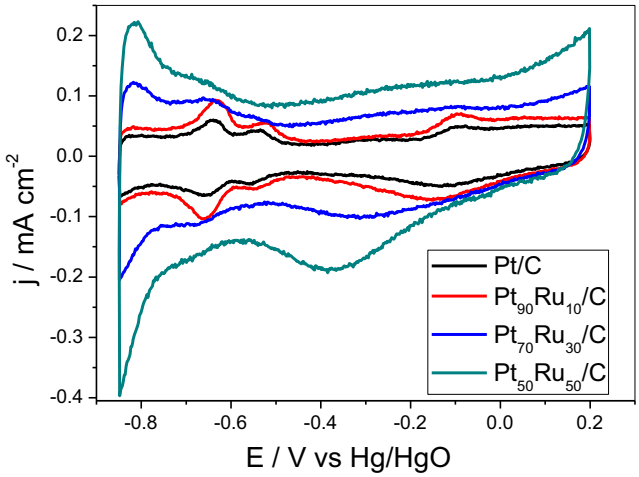

Fig. 4 Cyclic voltammograms of Pt/C and PtRu/C (90:10, 70:30, and 50:50) electrocatalysts in 1 mol L^{-1} KOH. Scan rate of 20 mV s^{-1}

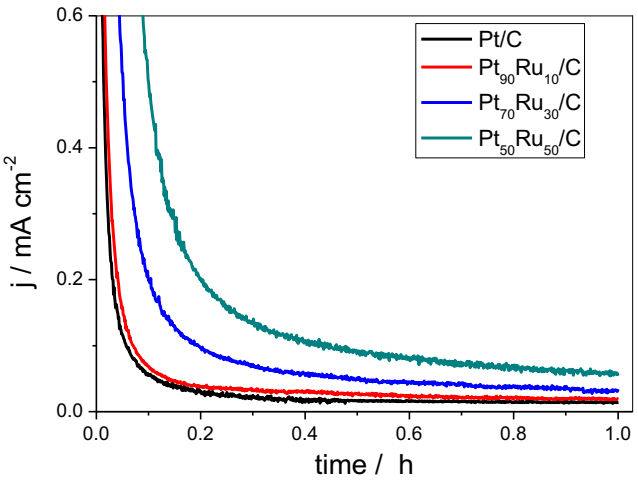

Fig. 6 Chronoamperometric measurements at − 0.35 V vs Hg/HgO on Pt/C and $Pt_{90}Ru_{10}$/C, $Pt_{70}Ru_{30}$/C, and $Pt_{50}Ru_{50}$/C electrocatalysts in 1 mol L^{-1} ethanol + 1 mol L^{-1} KOH

and Pt/C, respectively. Thus, it is evidenced that the presence of ruthenium promotes the Pt catalytic activity and reduces the onset potential of ethanol electrooxidation. In the forward scan, the highest peak current density for the ethanol oxidation process was also observed for $Pt_{50}Ru_{50}$/C. The trend of the peak current density on the forward scan was as follows: $Pt_{50}Ru_{50}$/C > $Pt_{70}Ru_{30}$/C > $Pt_{90}Ru_{10}$/C > Pt/C. Hu et al. [34] also reported better results for ethanol electrooxidation in alkaline media using PtRu catalysts than Pt catalysts. Based on the CV experiments in this study, $Pt_{50}Ru_{50}$/C is the most promising electrocatalyst for ethanol electrooxidation in alkaline media, which could be related to the presence of high amount of Ru and high amounts of RuO_2xH_2O on the catalyst surface as revealed by XPS analysis.

The chronoamperometry curves of all electrocatalysts for ethanol electrooxidation reaction at − 0.35 V for 60 min are shown in Fig. 6. The current density decreases continuously within the first several minutes and reaches the steady state after about 30 min. The gradual decay of current is associated with the accumulation of adsorbed species on the catalyst surface and surface passivation [2, 59]. The highest current density at the end of the experiment was observed for $Pt_{50}Ru_{50}$/C (about 3.9 times higher than that obtained using Pt/C) suggesting that this catalyst has good stability and is more tolerant to the poisoning species. In fact, the lowest current density after 1 h of experiment was obtained for Pt/C. The addition of Ru to Pt increases the current density and stability for ethanol electrooxidation. This is associated with the oxygenized species present on ruthenium during the ethanol electrooxidation process according to the bi-functional mechanism. In this mechanism, Ru atom interacts with hydroxyl to form Ru-OH at low potential in the alkaline media,

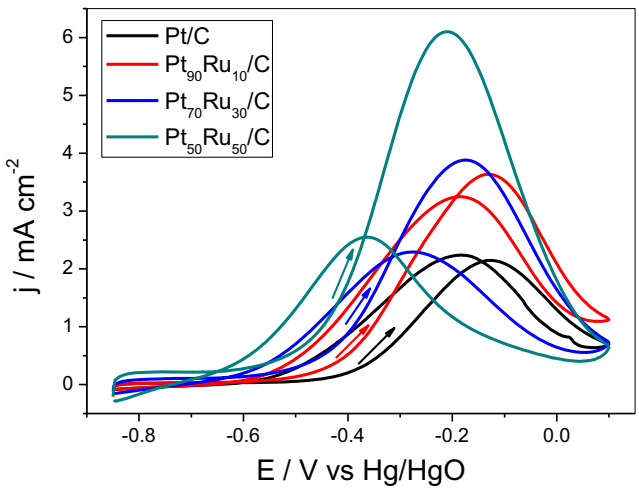

Fig. 5 Cyclic voltammograms of Pt/C and $Pt_{90}Ru_{10}$/C, $Pt_{70}Ru_{30}$/C, and $Pt_{50}Ru_{50}$/C electrocatalysts in 1 mol L^{-1} ethanol + 1 mol L^{-1} KOH. Scan rate of 20 mV s^{-1}

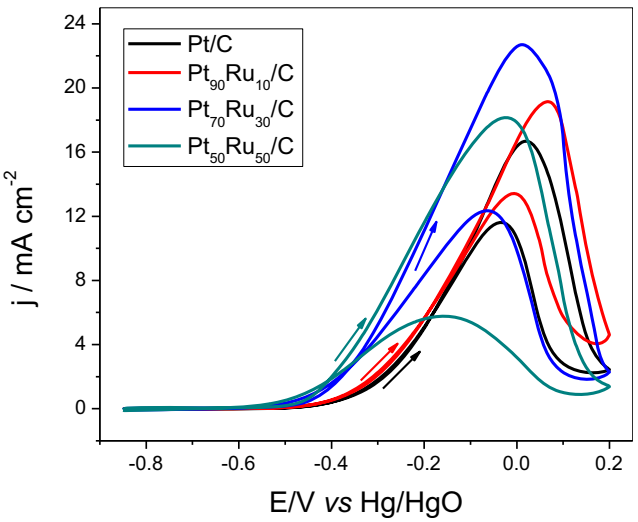

Fig. 7 Cyclic voltammograms of Pt/C and $Pt_{90}Ru_{10}$/C, $Pt_{70}Ru_{30}$/C, and $Pt_{50}Ru_{50}$/C electrocatalysts in 1 mol L^{-1} ethylene glycol + 1 mol L^{-1} KOH. Scan rate of 20 mV s^{-1}

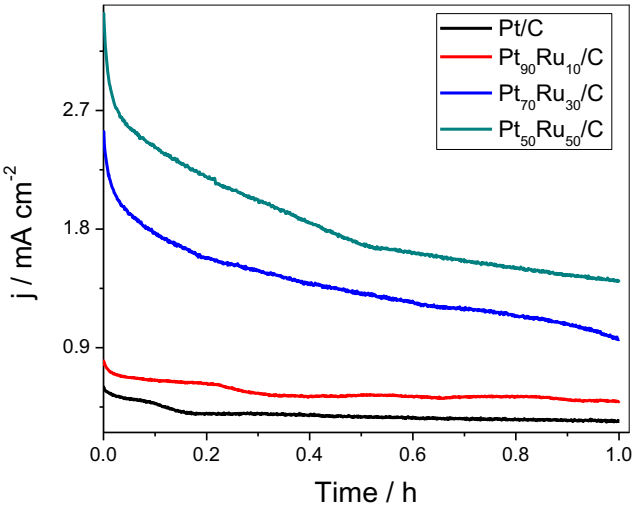

Fig. 8 Chronoamperometric measurements at − 0.35 V vs Hg/HgO on Pt/C and $Pt_{90}Ru_{10}$/C, $Pt_{70}Ru_{30}$/C, and $Pt_{50}Ru_{50}$/C electrocatalysts in 1 mol L^{-1} ethylene glycol + 1 mol L^{-1} KOH at room temperature

which enhance the electrooxidation of intermediates from ethanol oxidation reaction [34].

Ethylene Glycol Electrooxidation

Figure 7 shows the cyclic voltammograms of Pt_xRu_{100-x}/C ($x = 100$, 90, 70 and 50 at.%) in 1 mol L^{-1} KOH + 1 mol L^{-1} ethylene glycol. Similar to ethanol, higher Ru content lowers the onset potential for ethylene glycol oxidation. The lowest onset potential for ethylene glycol electrooxidation was obtained using $Pt_{50}Ru_{50}$/C. The values of onset potentials were about − 0.39 V, − 0.40 V, − 0.44 V, and − 0.46 V for pure Pt compositions of 100, 90, 70, 50 at. %, respectively. This is also consistent with previous literature reports [5, 10, 22]. The enhancement in the catalytic activity in the ethylene glycol process is related to the feature of Ru from Ru-OH at a low potential in the alkaline media, which increase the electrooxidation of adsorbed intermediates on Pt sites [34].

The best result obtained using $Pt_{50}Ru_{50}$/C in this study might be related to the higher amount of ruthenium and high amounts of RuO_2xH_2O oxygenized species on the catalyst surface as suggested by XPS analysis in this material, and consequently higher concentration of OH_{ads} promoted from ruthenium [6, 10, 60]. Similar to ethanol electrooxidation, the OH_{ads} species from Ru surface promote the ethylene glycol electrooxidation process [10]. The results show a clear increase in the catalyst performance for ethylene glycol electrooxidation with increasing the ruthenium amount in the materials.

The chronoamperometry curves of all electrocatalysts for ethylene glycol electrooxidation reaction at − 0.35 V for 60 min are shown in Fig. 8. The catalysts show the current density decline without reaching a steady state even after 1 h. This could be related to a decrease of the catalytic activity for ethylene glycol as can be seen in the literature [9, 10, 15]. The current density at the end of the experiment obtained using $Pt_{50}Ru_{50}$/C was ~ 327% higher than that using Pt/C. It is also possible to observe that the current density increases as the amount of ruthenium in the material increases. Therefore, it shows that ruthenium presents a positive effect with platinum towards ethylene glycol electrooxidation as also observed for ethanol. These results are in agreement with the literature in which is reported that PtRu/C shows higher catalytic activity towards ethylene glycol than Pt/C [5, 10].

Fuel Cell Performance Measurements

Our CV and CA experiments in ethanol and ethylene glycol containing solutions have shown that $Pt_{50}Ru_{50}$/C has the highest catalytic activity for both ethanol and ethylene glycol electrooxidation. Based on this finding, the fuel cell experiments fed with ethanol and ethylene glycol were performed

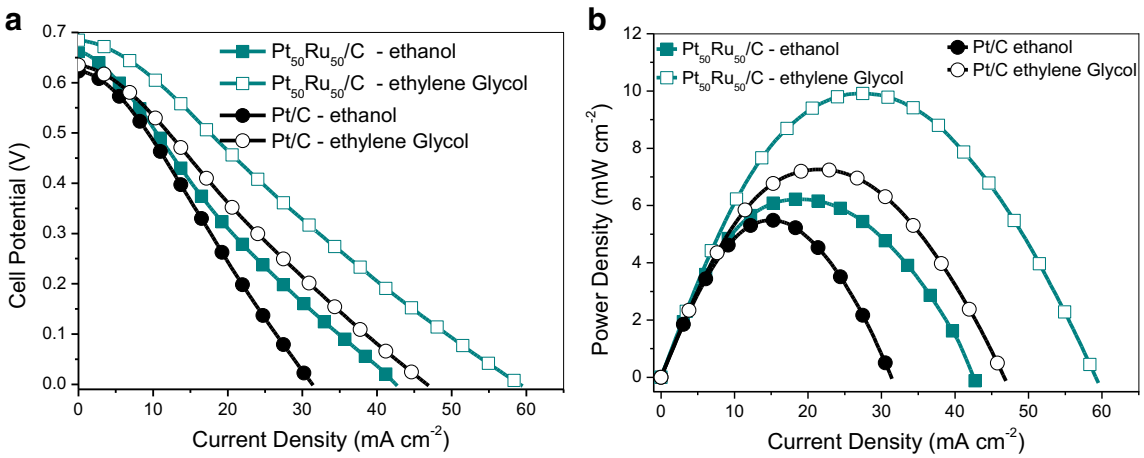

Fig. 9 Polarization curves (**a**) and the power density (**b**) at 70 °C of a 5 cm^2 fuel cell feed with ethanol and ethylene glycol using Pt/C and PtRu/C (50:50) electrocatalysts

with $Pt_{50}Ru_{50}$/C as anode, and the results were compared to that obtained using Pt/C as anode. Figure 9 shows the polarization curves using Pt/C and $Pt_{50}Ru_{50}$/C. The open-circuit voltage for ethanol (0.66 V) and ethylene glycol (0.68 V) on $Pt_{50}Ru_{50}$/C were higher compared to Pt/C, which were 0.62 V for ethanol and 0.63 V for ethylene glycol. From Fig. 8b was possible to observe that the maximum power density and current density were obtained using $Pt_{50}Ru_{50}$/C for ethanol and ethylene glycol. Thus, both fuel cell and electrochemical CV and CA experiments show the catalytic activity of $Pt_{50}Ru_{50}$/C for ethanol and ethylene glycol being much higher than Pt/C.

An important point that can be observed from CA, CV, and fuel cell experiments is that the current density for ethylene glycol electrooxidation were higher than for ethanol, for all electrocatalyst materials. This may be related to conversion of fuels to partially oxidized products, i.e., acetate in the case of ethanol and oxalate in the case of ethylene glycol. It must be noted that the oxidation of ethanol to acetate involves an exchange of four electrons per molecule of ethanol [17, 18], which corresponds to a Faradic efficiency of 33.3%. However, the oxidation of ethylene glycol in alkaline media to oxalate involves eight electrons per molecule of ethylene glycol, which corresponds to a Faradic efficiency of 80% [19, 20]. On the other hand, the complete oxidation of ethanol to CO_2 involves 12 electrons per molecule, and 10 electrons are released per molecule of ethylene glycol completely oxidized to CO_2 [5, 11]. It is important to stress that considering the acetate and oxalate as the main products from ethanol and ethylene glycol respectively, the K^+ ions from the KOH electrolyte probably form the organic salts with these compounds at the anode.

Conclusion

Our results show that the addition of Ru to Pt improves the catalytic activity of Pt towards ethanol and ethylene glycol electrooxidation in alkaline media. The XRD and XPS confirmed that PtRu alloy was formed for all bimetallic compositions. According to STEM analysis, the nanoparticle mean size are 7.3 nm, 5.7 nm, 5.2 nm, and 5.1 nm for Pt/C, $Pt_{90}Ru_{10}$/C, $Pt_{70}Ru_{30}$/C, and $Pt_{50}Ru_{50}$/C, respectively. Based in XPS analysis, $Pt_{50}Ru_{50}$/C has higher amount of Pt oxides on the surface than $Pt_{70}Ru_{30}$/C. Among different PtRu/C atomic ratios, the catalyst $Pt_{50}Ru_{50}$/C showed the best catalytic activity for both ethanol and ethylene glycol electrooxidation. For $Pt_{50}Ru_{50}$/C catalysts, we observed the lowest onset potential for ethanol (~ − 0.60 V) and ethylene glycol (~ − 0.46 V) electrooxidation, which are 160 and 70 mV lower than using Pt/C, respectively. In CA experiments, the current densities of ethanol and ethylene glycol electrooxidation at the end of the experiment were about 3.9 and 3.3 higher on $Pt_{50}Ru_{50}$/C than on Pt/C, and in the DAFC experiments showed that the maximum power density about 40% for ethanol and 14% higher than using Pt/C anode. The enhancement of the catalytic activity might be related to the high amount of oxides species on the PtRu electrocatalyst surface, the ability of ruthenium to atoms interacts with hydroxyl species to form Ru-OH at low potential which enhance the electrooxidation of intermediates from ethanol and ethylene glycol electrooxidation reaction and also due to the electronic effect of PtRu alloy that weakens the adsorption strength of poisonous intermediates from reactions on the catalyst surface. Furthermore, an electronic effect in PtRu alloy cannot be disregarded as it could play a role in improved catalytic activity of $Pt_{50}Ru_{50}$ material.

Acknowledgments The authors wish to thank FAPESP (Proc. no 2014/09087-4, 2014/09868-6) and CAPES for the financial support. Use of TEM facilities (JEOL JEM-2100F) of LNNano-CNPEM is greatly acknowledged.

References

1. C.-L. Sun, J.-S. Tang, N. Brazeau, J.-J. Wu, S. Ntais, C.-W. Yin, H.-L. Chou, E.A. Baranova, Particle size effects of sulfonated graphene supported Pt nanoparticles on ethanol electrooxidation. Electrochim. Acta **162**, 282–289 (2015)
2. J.C.M. Silva, B. Anea, R.F.B. De Souza, M.H.M.T. Assumpcao, M.L. Calegaro, A.O. Neto, M.C. Santos, J. Braz. Chem. Soc. **24**, 1553–1560 (2013)
3. N. Maffei, L. Pelletier, A. McFarlan, A high performance direct ammonia fuel cell using a mixed ionic and electronic conducting anode. J. Power Sources **175**(1), 221–225 (2008)
4. S.C. Zignani, V. Baglio, J.J. Linares, G. Monforte, E.R. Gonzalez, A.S. Aricò, Performance and selectivity of PtxSn/C electrocatalysts for ethanol oxidation prepared by reduction with different formic acid concentrations. Electrochim. Acta **70**, 255–265 (2012)
5. A. Falase, M. Main, K. Garcia, A. Serov, C. Lau, P. Atanassov, Electrooxidation of ethylene glycol and glycerol by platinum-based binary and ternary nano-structured catalysts. Electrochim. Acta **66**, 295–301 (2012)
6. J.M. Sieben, M.M.E. Duarte, Methanol, ethanol and ethylene glycol electro-oxidation at Pt and Pt–Ru catalysts electrodeposited over oxidized carbon nanotubes. Int. J. Hydrog. Energy **37**(13), 9941–9947 (2012)
7. J.F. Gomes, V.L. Oliveira, P.M.P. Pratta, G. Tremiliosi-Filho, Reactivity of alcohols with three-carbon atom chain on Pt in acidic medium. Electrocatalysis **6**(1), 7–19 (2015)
8. A.L. Ocampo, Q.-Z. Jiang, Z.-F. Ma, J.R. Varela, J. de Gyves, The effect of TiO2 on the catalytic activity of a PtRu/C catalyst for methanol oxidation. Electrocatalysis **5**(4), 387–395 (2014)
9. O.O. Fashedemi, K.I. Ozoemena, Comparative electrocatalytic oxidation of ethanol, ethylene glycol and glycerol in alkaline medium at Pd-decorated FeCo@Fe/C core-shell nanocatalysts. Electrochim. Acta **128**, 279–286 (2014)
10. H.J. Kim, S.M. Choi, S. Green, G.A. Tompsett, S.H. Lee, G.W. Huber, W.B. Kim, Highly active and stable PtRuSn/C catalyst for electrooxidations of ethylene glycol and glycerol. Appl. Catal. B Environ. **101**(3-4), 366–375 (2011)

11. A.O. Neto, S.G. da Silva, G.S. Buzzo, R.F.B. de Souza, M.H.M.T. Assumpção, E.V. Spinacé, J.C.M. Silva, Ethanol electrooxidation on PdIr/C electrocatalysts in alkaline media: electrochemical and fuel cell studies. Ionics **21**(2), 487–495 (2015)
12. M. Simões, S. Baranton, C. Coutanceau, Electro-oxidation of glycerol at Pd based nano-catalysts for an application in alkaline fuel cells for chemicals and energy cogeneration. Appl. Catal. B Environ. **93**(3-4), 354–362 (2010)
13. S.G. da Silva, J.C.M. Silva, G.S. Buzzo, R.F.B. De Souza, E.V. Spinacé, A.O. Neto, M.H.M.T. Assumpção, Electrochemical and fuel cell evaluation of PtAu/C electrocatalysts for ethanol electrooxidation in alkaline media. Int. J. Hydrog. Energy **39**(19), 10121–10127 (2014)
14. S.Y. Shen, T.S. Zhao, J.B. Xu, Carbon supported PtRh catalysts for ethanol oxidation in alkaline direct ethanol fuel cell. Int. J. Hydrog. Energy **35**(23), 12911–12917 (2010)
15. D. González-Quijano, W.J. Pech-Rodríguez, J.I. Escalante-García, G. Vargas-Gutiérrez, F.J. Rodríguez-Varela, Electrocatalysts for ethanol and ethylene glycol oxidation reactions. Part I: effects of the polyol synthesis conditions on the characteristics and catalytic activity of Pt–Sn/C anodes. Int. J. Hydrog. Energy **39**(29), 16676–16685 (2014)
16. S. Beyhan, K. Uosaki, J.M. Feliu, E. Herrero, Electrochemical and in situ FTIR studies of ethanol adsorption and oxidation on gold single crystal electrodes in alkaline media. J. Electroanal. Chem. **707**, 89–94 (2013)
17. L. Jiang, A. Hsu, D. Chu, R. Chen, Ethanol electro-oxidation on Pt/C and PtSn/C catalysts in alkaline and acid solutions. Int. J. Hydrog. Energy **35**(1), 365–372 (2010)
18. A.O. Neto, S.G. da Silva, G.S. Buzzo, R.F.B. de Souza, M.H.M.T. Assumpção, E.V. Spinacé, J.C.M. Silva, Ionics, 1–9 (2014)
19. W. Hauffe, J. Heitbaum, The electrooxidation of ethylene glycol at platinum in potassium hydroxide. Electrochim. Acta **23**(4), 299–304 (1978)
20. R.B. de Lima, V. Paganin, T. Iwasita, W. Vielstich, On the electrocatalysis of ethylene glycol oxidation. Electrochim. Acta **49**(1), 85–91 (2003)
21. E. Antolini, E.R. Gonzalez, Alkaline direct alcohol fuel cells. J. Power Sources **195**(11), 3431–3450 (2010)
22. Y. Feng, W. Yin, Z. Li, C. Huang, Y. Wang, Ethylene glycol, 2-propanol electrooxidation in alkaline medium on the ordered intermetallic PtPb surface. Electrochim. Acta **55**(23), 6991–6999 (2010)
23. J.M. Sieben, M.M.E. Duarte, Nanostructured Pt and Pt–Sn catalysts supported on oxidized carbon nanotubes for ethanol and ethylene glycol electro-oxidation. Int. J. Hydrog. Energy **36**(5), 3313–3321 (2011)
24. E.A. Baranova, M.A. Padilla, B. Halevi, T. Amir, K. Artyushkova, P. Atanassov, Electrooxidation of ethanol on PtSn nanoparticles in alkaline solution: correlation between structure and catalytic properties. Electrochim. Acta **80**, 377–382 (2012)
25. E.A. Monyoncho, S.N. Steinmann, P. Sautet, E.A. Baranova, C. Michel, Computational screening for selective catalysts: cleaving the C C bond during ethanol electro-oxidation reaction. Electrochim. Acta **274**, 274–278 (2018)
26. A. Dutta, S.S. Mahapatra, J. Datta, High performance PtPdAu nano-catalyst for ethanol oxidation in alkaline media for fuel cell applications. Int. J. Hydrog. Energy **36**(22), 14898–14906 (2011)
27. Y. Huang, J. Cai, Y. Guo, A high-efficiency microwave approach to synthesis of Bi-modified Pt nanoparticle catalysts for ethanol electro-oxidation in alkaline medium. Appl. Catal. B Environ. **129**, 549–555 (2013)
28. M.C. Figueiredo, R.M. Arán-Ais, J.M. Feliu, K. Kontturi, T. Kallio, Pt catalysts modified with Bi: Enhancement of the catalytic activity for alcohol oxidation in alkaline media. J. Catal. **312**, 78–86 (2014)
29. H. Li, G. Sun, L. Cao, L. Jiang, Q. Xin, Comparison of different promotion effect of PtRu/C and PtSn/C electrocatalysts for ethanol electro-oxidation. Electrochim. Acta **52**(24), 6622–6629 (2007)
30. F. Colmati, E. Antolini, E.R. Gonzalez, Effect of temperature on the mechanism of ethanol oxidation on carbon supported Pt, PtRu and Pt3Sn electrocatalysts. J. Power Sources **157**(1), 98–103 (2006)
31. N. Nakagawa, Y. Kaneda, M. Wagatsuma, T. Tsujiguchi, Product distribution and the reaction kinetics at the anode of direct ethanol fuel cell with Pt/C, PtRu/C and PtRuRh/C. J. Power Sources **199**, 103–109 (2012)
32. J. Thepkaew, S. Therdthianwong, A. Therdthianwong, A. Kucernak, N. Wongyao, Promotional roles of Ru and Sn in mesoporous PtRu and PtRuSn catalysts toward ethanol electrooxidation. Int. J. Hydrog. Energy **38**(22), 9454–9463 (2013)
33. Y. Hu, A. Zhu, Q. Zhang, Q. Liu, Preparation of PtRu/C core–shell catalyst with polyol method for alcohol oxidation. Int. J. Hydrog. Energy **41**(26), 11359–11368 (2016)
34. H. Xu, B. Yan, K. Zhang, J. Wang, S. Li, C. Wang, Y. Shiraishi, Y. Du, P. Yang, Eco-friendly and facile synthesis of novel bayberry-like PtRu alloy as efficient catalysts for ethylene glycol electrooxidation. Int. J. Hydrog. Energy **42**(32), 20720–20728 (2017)
35. P. Kanninen, M. Borghei, J. Hakanpää, E.I. Kauppinen, V. Ruiz, T. Kallio, Temperature dependent performance and catalyst layer properties of PtRu supported on modified few-walled carbon nanotubes for the alkaline direct ethanol fuel cell. J. Electroanal. Chem. **793**, 48–57 (2017)
36. R.F.B. De Souza, G.S. Buzzo, J.C.M. Silva, E.V. Spinacé, A.O. Neto, M.H.M.T. Assumpção, Effect of TiO2 content on ethanol electrooxidation in alkaline media using Pt nanoparticles supported on physical mixtures of carbon and TiO2 as electrocatalysts. Electrocatalysis **5**(2), 213–219 (2014)
37. J.C.M. Silva, G.S. Buzzo, R.F.B. De Souza, E.V. Spinacé, A.O. Neto, M.H.M.T. Assumpção, Enhanced electrooxidation of ethanol using Pd/C + TiO2 electrocatalysts in alkaline media. Electrocatalysis **6**(1), 86–91 (2015)
38. S. Hüfner, G.K. Wertheim, Core-line asymmetries in the x-ray-photoemission spectra of metals. Phys. Rev. B **11**(2), 678–683 (1975)
39. Q. Jiang, L. Jiang, J. Qi, S. Wang, G. Sun, Experimental and density functional theory studies on PtPb/C bimetallic electrocatalysts for methanol electrooxidation reaction in alkaline media. Electrochim. Acta **56**(18), 6431–6440 (2011)
40. M.H.M.T. Assumpção, S.G. da Silva, R.F.B. de Souza, G.S. Buzzo, E.V. Spinacé, A.O. Neto, J.C.M. Silva, Direct ammonia fuel cell performance using PtIr/C as anode electrocatalysts. Int. J. Hydrog. Energy **39**(10), 5148–5152 (2014)
41. H. Hou, S. Wang, W. Jin, Q. Jiang, L. Sun, L. Jiang, G. Sun, KOH modified Nafion112 membrane for high performance alkaline direct ethanol fuel cell. Int. J. Hydrog. Energy **36**(8), 5104–5109 (2011)
42. M.H.M.T. Assumpção, S.G. da Silva, R.F.B. De Souza, G.S. Buzzo, E.V. Spinacé, M.C. Santos, A.O. Neto, J.C.M. Silva, Investigation of PdIr/C electrocatalysts as anode on the performance of direct ammonia fuel cell. J. Power Sources **268**, 129–136 (2014)
43. T.L. Lomocso, E.A. Baranova, Electrochemical oxidation of ammonia on carbon-supported bi-metallic PtM (M=Ir, Pd, SnOx) nanoparticles. Electrochim. Acta **56**(24), 8551–8558 (2011)
44. J.C.M. Silva, S.G. da Silva, R.F.B. De Souza, G.S. Buzzo, E.V. Spinacé, A.O. Neto, M.H.M.T. Assumpção, PtAu/C electrocatalysts as anodes for direct ammonia fuel cell. Appl. Catal. A Gen. **490**, 133–138 (2015)
45. M.H.M.T. Assumpção, R.M. Piasentin, P. Hammer, R.F.B. De Souza, G.S. Buzzo, M.C. Santos, E.V. Spinacé, A.O. Neto, J.C.M. Silva, Appl. Catal. B Environ. **174–175**, 136–144 (2015)

46. W.H. Lizcano-Valbuena, V.A. Paganin, E.R. Gonzalez, Methanol electro-oxidation on gas diffusion electrodes prepared with Pt□Ru/C catalysts. Electrochim. Acta **47**(22-23), 3715–3722 (2002)
47. E.A. Baranova, Y. Le Page, D. Ilin, C. Bock, B. MacDougall, P.H.J. Mercier, Size and composition for 1–5nm Ø PtRu alloy nanoparticles from Cu Kα X-ray patterns. J. Alloys Compd. **471**(1-2), 387–394 (2009)
48. J.C.M. Silva, S. Ntais, É. Teixeira-Neto, E.V. Spinacé, X. Cui, A.O. Neto, E.A. Baranova, Evaluation of carbon supported platinum–ruthenium nanoparticles for ammonia electro-oxidation: combined fuel cell and electrochemical approach. Int. J. Hydrog. Energy **42**(1), 193–201 (2017)
49. R.J. Isaifan, S. Ntais, E.A. Baranova, Appl. Catal. A Gen. **464–465**, 87–94 (2013)
50. L.K. Ono, B. Roldan Cuenya, Formation and thermal stability of Au2O3on gold nanoparticles: size and support effects. J. Phys. Chem. C **112**(12), 4676–4686 (2008)
51. Y. Liang, J. Li, Q.-C. Xu, R.-Z. Hu, J.-D. Lin, D.-W. Liao, Characterization of composite carbon supported PtRu catalyst and its catalytic performance for methanol oxidation. J. Alloys Compd. **465**(1-2), 296–304 (2008)
52. A.S. Aricò, V. Baglio, A. Di Blasi, E. Modica, P.L. Antonucci, V. Antonucci, Analysis of the high-temperature methanol oxidation behaviour at carbon-supported Pt–Ru catalysts. J. Electroanal. Chem. **557**, 167–176 (2003)
53. E.A. Monyoncho, S. Ntais, F. Soares, T.K. Woo, E.A. Baranova, Synergetic effect of palladium–ruthenium nanostructures for ethanol electrooxidation in alkaline media. J. Power Sources **287**, 139–149 (2015)
54. B. Yang, Q. Lu, Y. Wang, L. Zhuang, J. Lu, P. Liu, J. Wang, R. Wang, Simple and low-cost preparation method for highly dispersed PtRu/C catalysts. Chem. Mater. **15**(18), 3552–3557 (2003)
55. A. Santasalo-Aarnio, S. Tuomi, K. Jalkanen, K. Kontturi, T. Kallio, The correlation of electrochemical and fuel cell results for alcohol oxidation in acidic and alkaline media. Electrochim. Acta **87**, 730–738 (2013)
56. L. Ma, D. Chu, R. Chen, Comparison of ethanol electro-oxidation on Pt/C and Pd/C catalysts in alkaline media. Int. J. Hydrog. Energy **37**(15), 11185–11194 (2012)
57. Y. Hu, A. Zhu, C. Zhang, Q. Zhang, Q. Liu, Microwave-assisted synthesis of double-shell PtRu/TiO2 catalyst towards methanol electro-oxidation. Int. J. Hydrog. Energy **40**(45), 15652–15662 (2015)
58. A.V. Tripković, S. Štrbac, K.D. Popović, Effect of temperature on the methanol oxidation at supported Pt and PtRu catalysts in alkaline solution. Electrochem. Commun. **5**(6), 484–490 (2003)
59. L. Ma, H. He, A. Hsu, R. Chen, PdRu/C catalysts for ethanol oxidation in anion-exchange membrane direct ethanol fuel cells. J. Power Sources **241**, 696–702 (2013)
60. M. Watanabe, S. Motoo, Electrocatalysis by ad-atoms. J. Electroanal. Chem. Interfacial Electrochem. **60**(3), 267–273 (1975)